Langmuir

Article

pubs.acs.org/Langmuir

Single Molecule Evidence for the Adaptive Binding of DOPA to Different Wet Surfaces

Yiran Li,[†] Meng Qin,[†] Ying Li,[‡] Yi Cao,*[,†] and Wei Wang*[,†]

[†]National Laboratory of Solid State Microstructure, Department of Physics, Nanjing University, 22 Hankou Road, Nanjing, Jiangsu, China 210093

[‡]Jiangsu Key Laboratory of Atmospheric Environment Monitoring & Pollution Control, Chemistry Department, School of Environmental Science & Engineering, Nanjing University of Information Science & Technology, Nanjing, Jiangsu, China 210044

Supporting Information

ABSTRACT: 3,4-Dihydroxyphenylalanine (DOPA) is the noncanonical amino acid widely found in mussel holdfast proteins, which is proposed to be responsible for their strong wet adhesion. This feature has also inspired the successful development of a range of DOPA-containing synthetic polymers for wet adhesions and surface coating. Despite the increasing applications of DOPA in material science, the underlying mechanism of DOPA−wet surface interactions remains unclear. In this work, we studied DOPA−surface interactions one bond at a time using atomic force microscope (AFM) based single molecule force spectroscopy. With our recently developed "multiple fishhook" protocol, we were able to perform high-throughput quantification of the binding strength of DOPA to various types of surfaces for the first time. We found that the dissociation forces between DOPA and nine different types of organic and inorganic surfaces are all in the range of 60−90 pN at a pulling speed of 1000 nm s^{-1}, suggesting the strong and versatile binding capability of DOPA to different types of surfaces. Moreover, by constructing the free energy landscape for the rupture events, we revealed several distinct binding modes between DOPA and different surfaces, which are directly related to the chemistry nature of the surfaces. These results explain the molecular origin of the versatile binding ability of DOPA. Moreover, we could quantitatively predict the relationship between DOPA contents and the binding strength based on the measured rupture kinetics. These serve as the bases for the quantitative prediction of the relationship between DOPA contents and adhesion strength to different wet surfaces, which is important for the design of novel DOPA based materials.

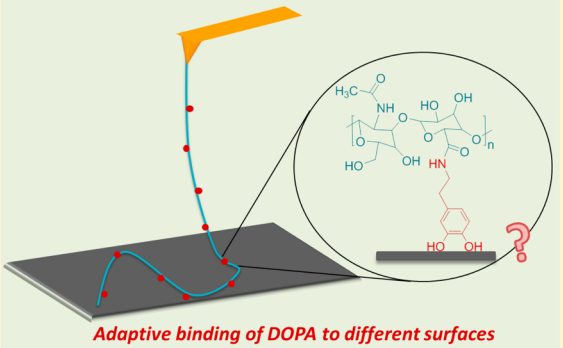

INTRODUCTION

A unique feature of marine mussels is their remarkable ability to stick to various wet surfaces.[1−3] Mussel adhesion is associated with the holdfast proteins secreted in the byssal plaque. Most of these holdfast proteins contain significant amount of 3,4-dihydroxyphenylalanine (DOPA), which is proposed to be responsible for their wet adhesion. This feature has also inspired the successful development of a range of DOPA-containing synthetic polymers for wet adhesions and surface coating techniques.[4−17] In spite of increasing applications of DOPA in material science, the underlying mechanism of DOPA−wet surface interactions remains unclear. The origin of such strong adhesion has been attributed to DOPA-mediated bidentate hydrogen bonding, coordinate bonding with metal/metal oxide, or covalent cross-linking.[18−21] Since the chemical properties of organic and inorganic surfaces are quite distinct, do these proteins utilize different binding mechanism for such diverse types of surfaces? What is the corresponding binding strength? Answering these questions is not only fundamentally important for the understanding of the adhesion mechanism of mussel holdfast proteins but also practically valuable for the design of new generation medical adhesives and coating materials.

In order to address these questions, the interactions of mussel holdfast proteins with various wet surfaces have been extensively studied using surface force apparatus (SFA).[17,20,22−27] Much information about the adhesion mechanism has been revealed. It was found that DOPA plays an important role in the wet adhesion. The adhesion strength is directly related to the DOPA contents and can be modulated through the protonation/deprotonation, redox, and metal chelation of the catechol group of DOPA. Although SFA can measure the macroscopic dissociation of two surfaces adhered by various mussel proteins, such measurement cannot clearly distinguish between cohesive and adhesive interactions. Moreover, these measurements utilize DOPA-containing proteins. The contribution from other amino acids of the proteins may complicate the interpretation of the DOPA−surface interactions. In contrast, atomic force spectroscopy (AFM) based single molecule force spectroscopy could allow the interactions

Received: March 28, 2014
Published: April 1, 2014

   dx.doi.org/10.1021/la501189n | *Langmuir* 2014, 30, 4358−4366

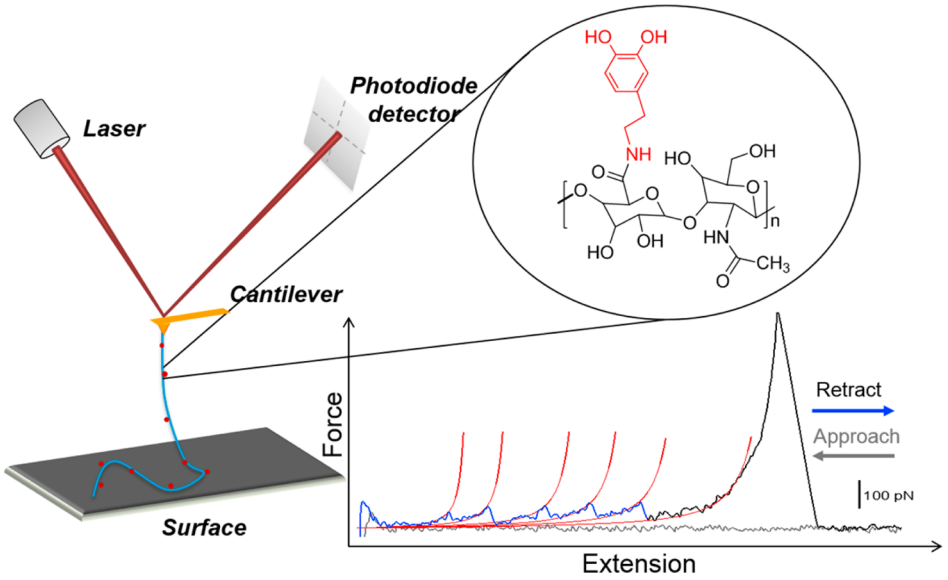

Figure 1. Scheme of single molecule AFM experiments on DOPA−surface interactions using the "multi-fishhook" approach. DOPA molecules (highlighted in red) were conjugated to hyaluronan (HA, colored in cyan) polymer through amide bonds. HA-DOPA molecules were incubated on various surfaces prior to each single-molecule pulling experiment. Then, the cantilever tip was brought into contact with the surface and pushing it with 2−3 nN to pick up HA-DOPA polymers by physically adsorbing HA-DOPA to the cantilever tip. Pulling a HA-DOPA polymer from the substrate surface results in the sequential rupture of DOPA−surface interactions. This gives rise to sawtooth-like traces (colored in blue) with each peak corresponding to a rupture event between DOPA and surface. These peaks can be adequately fitted using worm-like chain (WLC) models (red lines) with the same persistent length of ∼0.4 nm, indicating single molecule pulling events. The height of these peaks directly corresponds to the rupture force. Depending on whether the nonspecific interactions between HA-DOPA and the substrate surface is established, the last peak of the trace (colored in black) could either correspond to the specific DOPA−surface interaction or correspond to the detachment of nonspecifically adsorbed HA-DOPA from either the cantilever tip or the substrate surface, which typically occurs at much elevated forces.

between individual binding pairs being directly measured, from which the binding mechanisms can be inferred.[1,28−31] Directly measuring the interactions between DOPA and various surfaces at the single molecule level will allow the contributions of DOPA in mussel holdfast proteins to be understood quantitatively. Moreover, such measurements are also helpful for tailoring the DOPA contents of synthetic DOPA-containing polymer for optimum surface adhesions. A few pioneering single molecule AFM studies on DOPA−surface interactions have been conducted.[18,19] In these studies, DOPA was attached to the cantilever tip through a polymer linker or incorporated in a copolymer. Other amino acids were not included. However, due to the difficulties in performing single molecule force spectroscopy measurements, only titanium (or titanium dioxide) surface has been studies so far, and the results are not consistent probably due to different experimental conditions.[18,19] A more systematic study is required to fully address the interaction mechanism between DOPA and various wet surfaces.

Herein, we applied our recently developed "multiple-fishhook" approach[32] to measure the interactions between DOPA and surfaces (Figure 1). In this approach, multiple DOPA molecules are attached on a single polymer chain, hyaluronan (HA). Therefore, stretching each HA-DOPA molecule could result in many rupture events of single DOPA−surface interaction bonds, similar to the widely used polyprotein approach.[33−39] This method greatly increases the efficiency for obtaining sufficient high quality single-molecule data. Moreover, the nonspecific interactions and multiple unbinding events can be easily excluded in the data analysis. With this approach, we were able to quantitatively measure the interactions between DOPA and nine different surfaces systematically. We also performed pulling-speed-dependent experiments to unveil the free energy landscape underlying the dissociation of different types of DOPA−surface interactions. On the basis of these results, we revealed that DOPA can form several different types of interactions with various types of surfaces, which explains its versatile binding ability in wet conditions. Moreover, we could quantitatively predict the relationship between DOPA contents and the binding strength to different surfaces based on the measured rupture kinetics. We found that the binding strength increases rapidly at low DOPA contents and reaches half of the maximum binding strength generally in the range of 7−16% of DOPA. The increase of the binding strength becomes shallower at higher DOPA contents. Varying the amount of DOPA in mussel foot proteins allows tailoring their binding strength with various surfaces and under different environmental conditions. These results represent important concepts for the design of DOPA containing synthetic adhesives.

EXPERIMENTAL SECTION

Synthesis of HA-DOPA. To prepare the HA-DOPA conjugate, dopamine was coupled to the carboxyl group of HA by the EDC coupling reaction. First, 60.0 mg of HA (MW: 150 kDa; polydispersity: 1.4, Freda Biopharm, Shangdong, China) was dissolved in deionized water. Then 46.5 mg of EDC (Sigma-Aldrich) was add to the HA solution and stirred for 0.5 h. Next, 27.3 mg of dopamine was transferred into the EDC/HA solution to conjugate dopamine to HA. The reaction was conducted overnight at room temperature under magnetic stirring. The conjugate was purified by dialysis against excess Milli-Q water using dialysis tubing with the molecular weight cutoff of 50 kDa. The final product was lyophilized and stored at −20 °C for single molecule AFM experiments. The content of catechol in the molecule was determined by ^{1}H NMR.

dx.doi.org/10.1021/la501189n | *Langmuir* 2014, 30, 4358−4366

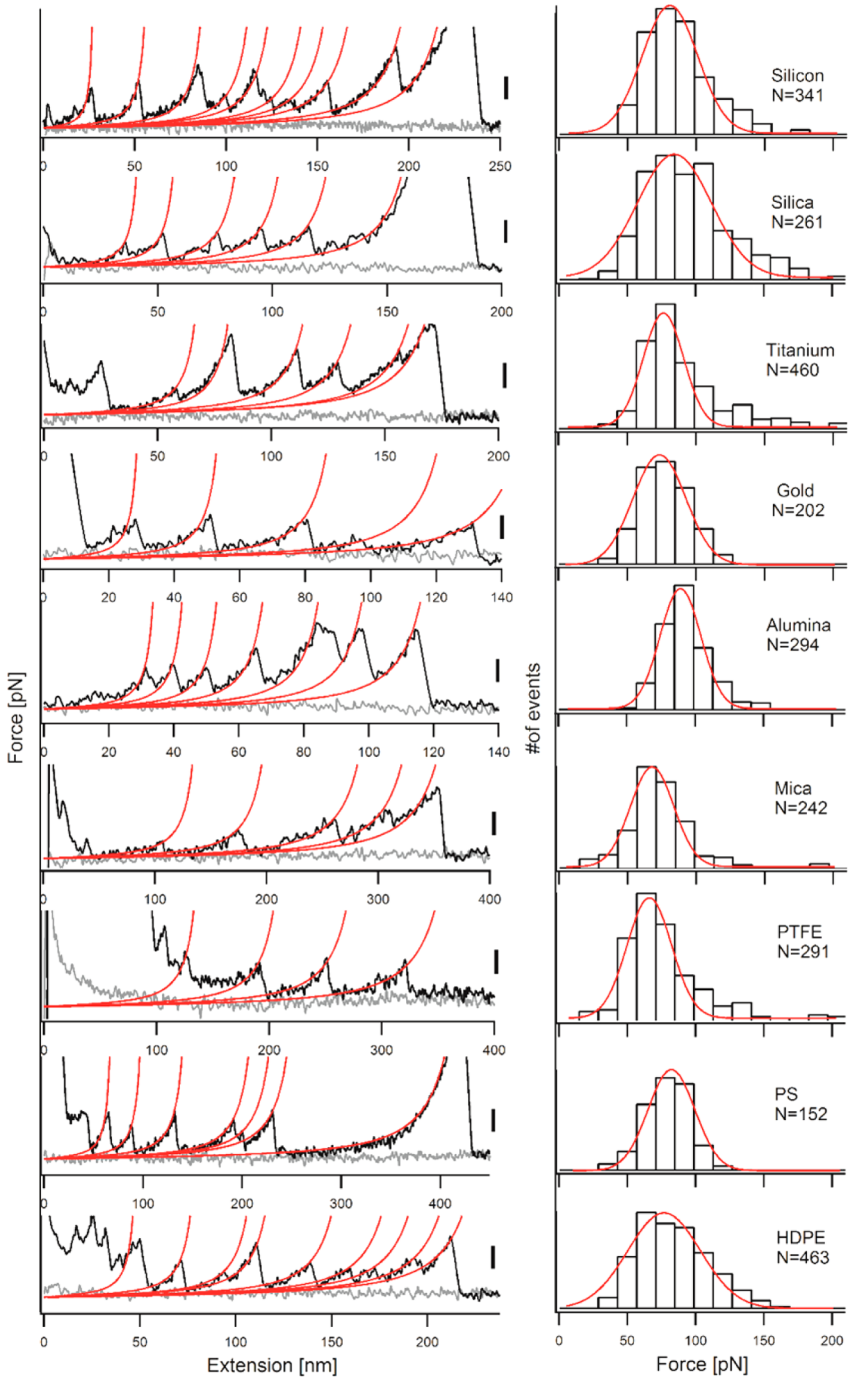

Figure 2. Single molecule force spectroscopy studies of DOPA–surface interactions. The left panel shows representative force–distance curves for the rupture of HA-DOPA with different substrates at a pulling speed of 1000 nm s^{-1}. Each peak corresponds to an individual rupture event between DOPA and the substrate. Red lines correspond to worm-like chain (WLC) fitting to the rupture events using the persistence length of 0.4 ± 0.1 nm. The scale bar on the right side of each curve represents 50 pN. The histograms for rupture forces for the same substrates are shown in parallel in the right panel. Red lines correspond to a Gaussian fit. HDPE = high-density polyethylene, PTFE = polytetrafluoroethene, and PS = polystyrene.

Substrate Preparation. All substrates were first cleaned ultrasonically in water and ethanol for 10 min. Then the inorganic substrates were further cleaned through the treatment with UV-ozone cleaner and chromic acid to remove the impurities and generate hydroxyl on the substrate surface. Next, several drops (~50–200 μL) of HA-DOPA solution (0.2 mg mL^{-1}) were spread on each substrate using pipet tip or a spin-coater. The substrates were stored in Tris buffer at 4 °C until use.

AFM Force Spectroscopy Experiments. AFM force spectroscopy experiments were carried out on a commercial AFM (JPK Nanowizard II). The force–distance curves were recorded by commercial software from JPK and analyzed by custom-written procedures in Igor pro 6.0 (Wavemetrics, Inc.). Before each force spectroscopy experiment, the substrate was extensively rinsed by Milli-Q water to remove floating HA-DOPA polymers. Next the fluid chamber was filled in with 1.5 mL of buffer containing 100 mM Tris·HCl and 50 mM NaCl at pH 7.2. AFM experiments were conducted after allowing the system to equilibrate for 30 min. AFM silicon nitride cantilevers with silicon nitride tips (type MLCT, from Bruker) were used in all experiments. The spring constants of the tips, calibrated by the thermal fluctuation method, were in the range of 0.037–0.057 N m^{-1}. We also used gold-coated AFM cantilevers (type Biolever BL-

dx.doi.org/10.1021/la501189n | *Langmuir* 2014, 30, 4358–4366

RC150VB, from Olympus) and silicon nitride cantilevers with silicon tips (type SNL, from Bruker) for control experiments. All AFM force measurements were carried out at 25 ± 1 °C.

RESULTS AND DISCUSSION

"Multiple Fishhook" Single Molecule Pulling Experiments. We first synthesized a HA polymer grafted with 11% DOPA (DOPA: carboxyl groups of HA = 11%) for single molecule force spectroscopy measurement (Figure S1 and Experimental Section). The carboxyl groups of HA were first converted to amine-reactive *O*-acylisourea intermediates with EDC. Then, these intermediates were reacted with dopamine to produce the final HA-DOPA polymer. The successful conjugation of DOPA was confirmed by ^{1}HNMR (Figure S2). As DOPA is prone to be oxidized in air, before each AFM experiment, the HA-DOPA polymer was reduced using ascorbic acid and the reduced DOPA was confirmed by UV spectra (Figure S3).[40]

Then we measured the rupture of DOPA−surface interactions using single molecule AFM. We immobilized HA-DOPA polymers on various surfaces prewetted by Tris buffer (100 mM, pH 7.2, containing 50 mM NaCl and 1 mM of ascorbic acid) for 15−30 min. In a typical experiment, the cantilever was brought to the surface with a constant speed of 1000 nm s^{-1} and held on the surface at constant forces of 2−3 nN for 1 s to allow the HA-DOPA molecules physically absorbed on the cantilever tip. We kept the pickup rate as low as ∼0.5% by adjusting the amount of HA-DOPA on the surface. Then the cantilever was moved back at the same speed to break DOPA−surface interactions. The typical experimental scenarios are depicted in Figure S4. The representative force−extension curves from various substrates are shown in Figure 2, left panel. These traces are in sawtooth-like shape with each peak corresponding to a rupture event of individual DOPA−surface interactions. Red lines are worm-like chain (WLC) fits to each individual peak. All peaks in the same trace can be fitted using a fixed persistence length of ∼0.4 nm, which is consistent with the persistence length of HA reported in the literature.[32] This confirmed that only single HA molecules were picked up. If multiple HA-DOPA molecules were picked up in the experiments, the resulting persistence length should be much smaller, and these data can be easily rejected. The spaces between individual peaks varied in a wide range because DOPA was grafted to HA randomly. Moreover, HA-DOPA adopted random-coil conformation in solution before being deposited to the surfaces. Because of the geometric hindrance, not all DOPA groups were accessible to the substrate surfaces. On the basis of the typical peak-to-peak distance of 30−50 nm of the single-molecule traces and the graft density of DOPA, we can infer that ∼1/5 of DOPA on the HA-DOPA molecules were adhered to the surface in our experiments. To further confirm that the sawtooth peaks were resulted from the rupture of DOPA−surface interactions, we performed control experiments using unmodified HA, HA-tyramine, and periodate-treated HA-DOPA. Tyramine contains only one phenol group; hence, its interaction with titanium surfaces is weaker than that of DOPA. Similarly, after the oxidation of the catechol group of DOPA to *o*-quinone, the binding of DOPA to titanium surfaces is prohibited. If the measured force peaks correspond to the rupture of nonspecific DOPA−surface interaction, we should not observe similar sawtooth-like patterns using HA-tyramine and periodate-treated HA-DOPA. Indeed, in these experiments, no such sawtooth-like curves were observed (Figures S5−S7). In our experimental design, we rely on nonspecific adhesions of HA-DOPA to cantilever tip to pick up HA-DOPA and rupture DOPA−surface interactions. It is important to make sure such nonspecific adsorption is stronger than a single DOPA-surface bond. Indeed, such nonspecific adhesion forces between HA and the cantilever tip can be as high as ∼300 pN, higher than the dissociation forces of the single DOPA-surface bond (Figure S8). We have tested three different types of cantilever tip materials (Si_3N_4, silicon, and gold). The nonspecific adhesion forces between HA and the cantilever tips were consistently higher than the rupture forces of DOPA−surface bonds (Figure S8). In our experimental design, DOPA in principle can also form specific bonds with cantilever tip. However, because the cantilever tip is typically very sharp with a tip radius less than 10 nm, such DOPA−tip bonds are minimized. To estimate whether trace amount of DOPA−tip interactions will affect the final results, we measured the rupture of HA-DOPA with gold surface using gold coated cantilever tip and the rupture of HA-DOPA with silicon surface using a silicon cantilever tip. Such "symmetric" experimental design ensures that the rupture events solely correspond to the DOPA−gold or DOPA−silicon interactions. Our experimental results indicated that no significant difference between the data measured using Si_3N_4 cantilever tips and those from such "symmetric" experiments (Figure S9). Furthermore, we have also used different types of cantilever tips (Si_3N_4, gold coated, and silicon) to measure the ruptures of HA-DOPA with the titanium surface. The rupture forces are independent of the types of cantilever tips (Figure S10). To further validate our approach, we studied the DOPA−titanium surface interactions using the traditional single molecule force spectroscopy approach, in which a single DOPA molecule was flanked to cantilever tip by a poly(ethylene glycol) (PEG) linker.[18,19,41] The representative traces and the rupture force histograms are shown in Figure S11. It is obvious that the two force histograms are superimposable. Therefore, the new approach could provide accurate rupture force measurement with much improved efficiency.

Subsequently, we analyzed the rupture forces on different surfaces. This could provide a direct comparison of the interaction strength of DOPA with different types of surfaces. The rupture force histograms at a pulling speed of 1000 nm s^{-1} are shown in Figure 2, right panel. Depending on different surfaces, the rupture forces are in the range of 30−200 pN with a broad distribution. The surface of the highest rupture force is silicon and that of the lowest is polytetrafluoroethene (PTFE). It seems that the rupture forces for both metal/metal oxide surfaces and other inorganic surfaces are very similar, indicating that DOPA is adaptive for the adsorption to diverse types of surfaces. However, the mechanism underlying such strong and adaptive binding is intriguing.

Free Energy Landscape for the Rupture of Different DOPA−Surface Bonds. To decipher the binding mechanism, we further investigated the free energy landscape underlying the rupture of different DOPA−surface interactions. Because the rupture of DOPA−surface bonding is a nonequilibrium process, the rupture force depends on the loading rate, r.[42] The higher the force loading rate, the larger the rupture force is. Simply comparing the rupture force at a given pulling speed cannot yield the information on the strength of each interaction. To this extent, we measured the rupture forces on different surfaces at various loading rates by simply adjusting the pulling speeds (Figure 3). Using the widely used Bell−Evans model,[43,44] we

dx.doi.org/10.1021/la501189n | *Langmuir* 2014, 30, 4358−4366

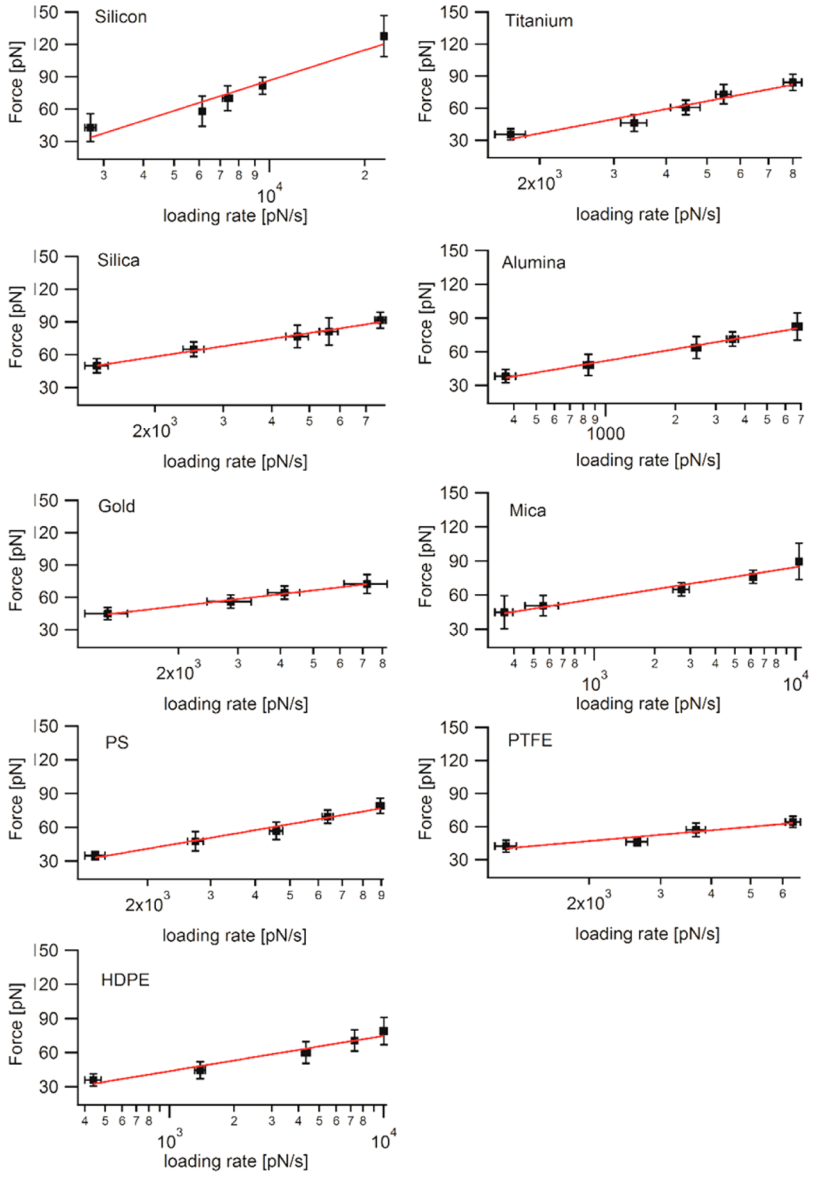

Figure 3. Loading-rate dependence for the rupture forces between the HA-DOPA and different substrates. Red lines correspond to the fits by the Bell–Evans model.

quantified the free energy barrier (ΔG) for the unbinding and the distance of the transition state or rupture distance (Δx).

$$F = \frac{k_B T}{\Delta x} \ln\left(\frac{\Delta x}{k_0 k_B T}\right) + \frac{k_B T}{\Delta x} \ln(r) \quad (1)$$

where F is the most probable rupture force, k_B is the Boltzmann constant, T is the absolute temperature, and k_0 is the spontaneous dissociation rate of the bond. The free energy barrier can be calculated as follows:

$$\Delta G = RT \ln(k_0/A) \quad (2)$$

where R is the gas constant and A is the Arrhenius prefactor or the frequency factor. We chose A of 10^6 s^{-1} in our calculation. The kinetic parameters for the rupture of interactions between DOPA and various surfaces are summarized in Table S1. Interestingly, although the rupture forces of DOPA with plastic surfaces are significantly lower than those with inorganic ones at the pulling speed of 1000 nm s^{-1}, the free energy barrier is almost the same. The lower rupture forces are mainly due to the longer distance to the transition state. It is worth mentioning that the rupture distance measured here is not related to the bond length, and ΔG is also not the bond strength. Bond length is the average distance between the centers of the nuclei of two bonded atoms in a molecule. However, the rupture distance is the length difference between bonded state and the rupture transition state. Similarly, the ΔG is also not bond energy but the barrier height for the rupture of a bond by force in aqueous solution. Bond energy is the thermodynamic energy, which depends on the relative energy between the bonded state and the dissociated state. However, the ΔG for the rupture of a bond by force is the kinetic energy, which depends on the free energy difference of the bond state and the transition state. Such a barrier depends on the reaction pathway. Moreover, the absolute value of ΔG is largely determined by the value of the Arrhenius prefactor, A, which was chosen as in the range of 10^6–10^9.[45,46] However, the relative scale of ΔG calculated using eq 2 is independent of A.

dx.doi.org/10.1021/la501189n | Langmuir 2014, 30, 4358–4366

Binding Mechanisms of DOPA with Various Surfaces. On the basis of the free energy landscape for the DOPA dissociation and the chemical properties of different types of surfaces, we are able to infer the possible binding mechanism. The ruptures of many different kinds of interactions have been studied extensively using force spectroscopy techniques (Figure 4).[31,47−59] Generally, the rupture of covalent bonds is of the shortest rupture distance of about 0.0007 nm but the highest free energy barrier of ∼50 kJ mol^{-1}. The rupture of electrostatic interactions shows a bit longer rupture distances of ∼0.04 nm, indicating potential well for charge−charge interactions is also quite steep. It is worth mentioning that the literature data for the rupture distances for charge−charge interactions may be a bit underestimated. Typical charge−charge interactions are not stable in water and prone to dissociation spontaneously. The two literature data were either measured inside biomolecule or from strong charge transfer complexes.[54,55] The rupture of coordinate bonds shows even longer rupture distance of ∼0.12 nm and similar free energy barrier. The hydrophobic interactions show much longer rupture distance while the free energy barrier is comparable with that of coordinate bond. Both the free energy and the rupture distance for the break of hydrogen bonds span a wide range, depending on the chemical environments of the hydrogen bonds. There are big overlaps between hydrophobic interactions and hydrogen bonds. However, as the criteria for the formation of hydrogen bonds are very stringent, the hydrogen bonds are only limited to hydrogen atoms bound to a highly electronegative atom, such as nitrogen, oxygen, or fluorine. With the knowledge of the chemical properties of the surfaces, we should be able to discriminate them unambiguously. Therefore, this plot provides a caliber for us to understand the nature of DOPA−surface interactions.

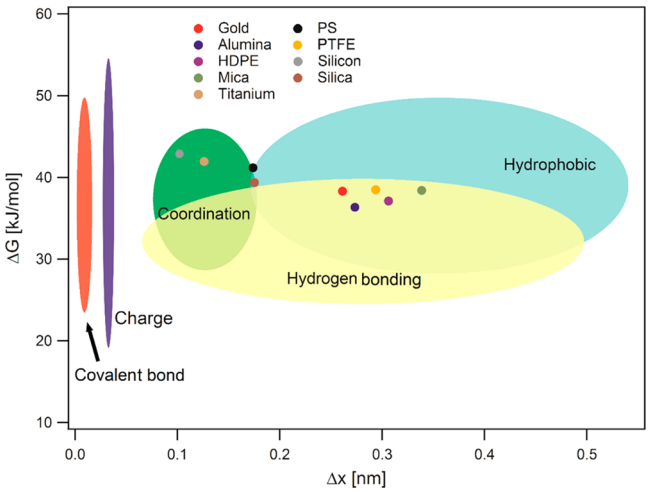

Figure 4. Free energy barrier (ΔG) versus rupture distance (Δx) plot for various types of interactions. ΔG and Δx of DOPA−surface interactions were calculated using the Bell−Evans model. The ellipses in the figure are calculated based on the data from previously published papers, which studied different types of chemical interactions. The covalent bond data were taken from refs 55, 57, coordination from refs 49−51, 59, hydrophobic interactions from refs 31, 47, 48, and hydrogen bonding from refs 52, 53. The size of the ellipses corresponds to the standard deviation of the literature data. In these literatures, different kinetic models or different Arrhenius prefactors may be used. To make the data consistent, the data were reanalyzed using the Bell−Evans model with an Arrhenius prefactor of 10^6. Clearly, DOPA may adopt several different kinds of binding modes with different substrates.

We also plot the free energy and rupture distance of DOPA from different surfaces in Figure 4. Clearly, none of these interactions are in the range of covalent bond or electrostatic interactions. Therefore, we believe that the coordinate bonds, hydrogen bonds, and hydrophobic interactions are the three possible mechanisms that DOPA utilized for surface binding. As expected, DOPA uses its catechol group to bind with titanium and silicon surfaces by forming coordinate bonds, and for silica surface, DOPA may prefer to form hydrogen bonds with oxygen atoms of the substrate or a hydrogen bond and another coordinate bond with silica. Therefore, the binding between DOPA and silica appears in the cross of hydrogen and coordination interactions. For hydrophobic surfaces, such as gold, PTFE, and high-density polyethylene (HDPE), with no surprise, they are in the range of hydrophobic area. Interestingly, the polystyrene (PS) and mica substrates show abnormal behavior. The rupture distance of PS substrate is much smaller than other plastic surfaces. We propose that this is due to the $\pi-\pi$ stacking between the catechol groups of DOPA and the phenyl groups of polystyrene. Mica is a compound containing both alumina and silica. The position of mica in Figure 3 is closer to alumina; so we propose that the chemical interaction between DOPA and mica is more likely by the hydrogen bond between the hydroxyl groups of DOPA and the oxygen atoms on alumina instead of coordinate bonding. Although different binding mechanisms between DOPA and various surfaces have been speculated from the SFA data, it fails to provide clear distinctions between different binding modes. Interestingly, a recent SFA study showed that DOPA-deficient foot protein of green mussels also possesses strong adhesion capability.[60] Single molecule force spectroscopy is complementary to the widely used SFA technique and allows deciphering the molecular binding mechanisms between DOPA and various surfaces. Our results indicate that the versatile binding capability of DOPA containing mussel holdfast proteins is mainly due to the adaptive binding mechanism between DOPA and different surfaces instead of the contributions from other amino acids.

Estimation of the Binding Strength of DOPA Containing Polymers with Various Surfaces. The kinetic parameters obtained in this study also allow us to estimate the work that is required to pull off DOPA-containing polymers from various surfaces. We used a Monte Carlo simulation procedure to generate the force−extension traces of rupturing single DOPA-containing polymers (i.e., HA-DOPA) with various DOPA contents (Figure S12). With the increase of DOPA contents, the force−extension traces turn from sawtooth-like shape to force plateaus, which is consistent with that reported previous by Wang et al.[19] Integrating the force−extension curves yields the work that is required to dissociate DOPA-containing polymers from various surfaces. Because we assumed all DOPA molecules bound to surfaces in our simulation, the calculated work should be considered as the upper limit of the binding energy. The amount of work increases with respect to the DOPA contents. However, the maximum work (at 100% DOPA) is different for various surfaces (Table S2). The inorganic surfaces, such as silicon, titanium, silica, and mica, show the strongest DOPA−surface interactions. The plastic surfaces, such as HDPE and PTFE, are of weaker binding strengths. Because DOPA cannot form hydrogen bonds or coordinate bonds with gold surface,

dx.doi.org/10.1021/la501189n | Langmuir 2014, 30, 4358−4366

DOPA−gold interactions are also hydrophobic in nature and similar to DOPA−plastic surface interactions. However, due to the presence of $\pi-\pi$ interactions, DOPA−PS interactions are notably stronger than other organic surfaces. More interestingly, the dissociation work shows a nonlinear relationship with the amount of DOPA in the polymers. At low DOPA contents, the dissociation work increases abruptly, while at high DOPA contents, the dissociation work gradually reaches a plateau (Figure S12). The content of DOPA that is required to reach the half of the maximum dissociation work (at 100% of DOPA) for each surface was summarized in Table S2. For all surfaces, 7−16% of DOPA is sufficient to provide half of the dissociation work with 100% of DOPA. Although increasing the amount of DOPA could increase the overall binding strength, the contribution from each DOPA group actually becomes less. There is much room for tailoring the binding strength of DOPA-containing polymers to various surfaces and under different environmental conditions by adjusting the DOPA contents. The rupture kinetics measured in this study may serve as an important reference for the design of DOPA containing synthetic adhesives.

CONCLUSION

In summary, we studied the interactions between DOPA and various surfaces at the single molecule level using the "multiple fishhook" force spectroscopy technique. We found that DOPA shows similar rupture forces of 60−90 pN to nine different surfaces, demonstrating the versatile binding ability of DOPA. Moreover, by quantifying the free energy landscape for the dissociation of DOPA to these surfaces, we were able to directly decipher their different binding modes. For example, our results suggested that DOPA might bind to mica by the hydrogen bond between the hydroxyl groups of DOPA and the oxygen atoms on alumina instead of coordination interactions with silica. Such mechanisms cannot be predicted from the chemistry nature of the surfaces a priori. Therefore, this study represents an important step toward the understanding of mussel adhesion mechanism. Based on this technique, many complex features of DOPA binding can be revealed. Studying the effect of chemical and biological environments of mussel holdfast proteins on the DOPA surface interactions will be our next endeavor.

ASSOCIATED CONTENT

Supporting Information

^{1}H NMR and UV−vis spectrum of HA-DOPA, control force spectroscopy experiments, and supporting tables. This material is available free of charge via the Internet at http://pubs.acs.org.

AUTHOR INFORMATION

Corresponding Authors

*Fax (+86) 25 83595535; e-mail caoyi@nju.edu.cn (Y.C.).

*Fax (+86) 25 83595535; e-mail wangwei@nju.edu.cn (W.W.).

Author Contributions

Y.L. and M.Q. contributed equally.

Notes

The authors declare no competing financial interest.

ACKNOWLEDGMENTS

This work was supported by the National Natural Science Foundation of China under Grants 11074115, 11334004, 31170813, and 91127026, the program for New Century Excellent Talents in University, and the Priority Academic Program Development of Jiangsu Higher Education.

ABBREVIATIONS

AFM, atomic force microscopy; SMFS, single-molecule force spectroscopy; DOPA, 3,4-dihydroxyphenylalanine; HA, hyaluronan; WLC, worm-like chain.

REFERENCES

(1) Even, M. A.; Wang, J.; Chen, Z. Structural information of mussel adhesive protein Mefp-3 acquired at various polymer/Mefp-3 solution interfaces. *Langmuir* **2008**, *24* (11), 5795−5801.

(2) Floriolli, R. Y.; von Langen, J.; Waite, J. H. Marine surfaces and the expression of specific byssal adhesive protein variants in Mytilus. *Mar. Biotechnol.* **2000**, *2* (4), 352−363.

(3) Waite, J. H.; Andersen, N. H.; Jewhurst, S.; Sun, C. J. Mussel adhesion: Finding the tricks worth mimicking. *J. Adhes.* **2005**, *81* (3−4), 297−317.

(4) Lee, H.; Dellatore, S. M.; Miller, W. M.; Messersmith, P. B. Mussel-inspired surface chemistry for multifunctional coatings. *Science* **2007**, *318* (5849), 426−430.

(5) Lee, H.; Lee, B. P.; Messersmith, P. B. A reversible wet/dry adhesive inspired by mussels and geckos. *Nature* **2007**, *448* (7151), 338−U4.

(6) Ye, Q.; Zhou, F.; Liu, W. M. Bioinspired catecholic chemistry for surface modification. *Chem. Soc. Rev.* **2011**, *40* (7), 4244−4258.

(7) Matos-Perez, C. R.; White, J. D.; Wilker, J. J. Polymer composition and substrate influences on the adhesive bonding of a biomimetic, cross-linking polymer. *J. Am. Chem. Soc.* **2012**, *134* (22), 9498−9505.

(8) Krogsgaard, M.; Behrens, M. A.; Pedersen, J. S.; Birkedal, H. Self-healing mussel-inspired multi-pH-responsive hydrogels. *Biomacromolecules* **2013**, *14* (2), 297−301.

(9) Garcia-Fernandez, L.; Cui, J.; Serrano, C.; Shafiq, Z.; Gropeanu, R. A.; San Miguel, V.; Ramos, J. I.; Wang, M.; Auernhammer, G. K.; Ritz, S.; Golriz, A. A.; Berger, R.; Wagner, M.; del Campo, A. Antibacterial strategies from the sea: Polymer-bound Cl-catechols for prevention of biofilm formation. *Adv. Mater.* **2013**, *25* (4), 529−533.

(10) Saiz-Poseu, J.; Sedo, J.; Garcia, B.; Benaiges, C.; Parella, T.; Alibes, R.; Hernando, J.; Busque, F.; Ruiz-Molina, D. Versatile nanostructured materials via direct reaction of functionalized catechols. *Adv. Mater.* **2013**, *25* (14), 2066−2070.

(11) Anderson, T. H.; Yu, J.; Estrada, A.; Hammer, M. U.; Waite, J. H.; Israelachvili, J. N. The contribution of DOPA to substrate-peptide adhesion and internal cohesion of mussel-inspired synthetic peptide films. *Adv. Funct. Mater.* **2010**, *20* (23), 4196−4205.

(12) Lee, H.; Lee, Y.; Statz, A. R.; Rho, J.; Park, T. G.; Messersmith, P. B. Substrate-independent layer-by-layer assembly by using mussel-adhesive-inspired polymers. *Adv. Mater.* **2008**, *20* (9), 1619−1623.

(13) Lee, Y.; Lee, H.; Kim, Y. B.; Kim, J.; Hyeon, T.; Park, H.; Messersmith, P. B.; Park, T. G. Bioinspired surface immobilization of hyaluronic acid on monodisperse magnetite nanocrystals for targeted cancer imaging. *Adv. Mater.* **2008**, *20* (21), 4154−4157.

(14) Lee, B. P.; Messersmith, P. B.; Israelachvili, J. N.; Waite, J. H.; Clarke, D. R.; Fratzl, P. Mussel-inspired adhesives and coatings. *Annu. Rev. Mater. Res.* **2011**, *41*, 99−132.

(15) Lee, H.; Rho, J.; Messersmith, P. B. Facile conjugation of biomolecules onto surfaces via mussel adhesive protein inspired coatings. *Adv. Mater.* **2009**, *21* (4), 431−434.

(16) Heo, J.; Kang, T.; Jang, S. G.; Hwang, D. S.; Spruell, J. M.; Killops, K. L.; Waite, J. H.; Hawker, C. J. Improved performance of protected catecholic polysiloxanes for bioinspired wet adhesion to surface oxides. *J. Am. Chem. Soc.* **2012**, *134* (49), 20139−20145.

(17) Yu, J.; Kan, Y.; Rapp, M.; Danner, E.; Wei, W.; Das, S.; Miller, D. R.; Chen, Y.; Waite, J. H.; Israelachvili, J. N. Adaptive hydrophobic and hydrophilic interactions of mussel foot proteins with organic thin films. *Proc. Natl. Acad. Sci. U. S. A.* **2013**, *110* (39), 15680−5.

(18) Lee, H.; Scherer, N. F.; Messersmith, P. B. Single-molecule mechanics of mussel adhesion. *Proc. Natl. Acad. Sci. U. S. A.* **2006**, *103* (35), 12999−13003.
(19) Wang, J. J.; Tahir, M. N.; Kappl, M.; Tremel, W.; Metz, N.; Barz, M.; Theato, P.; Butt, H. J. Influence of binding-site density in wet bioadhesion. *Adv. Mater.* **2008**, *20* (20), 3872−3875.
(20) Lin, Q.; Gourdon, D.; Sun, C. J.; Holten-Andersen, N.; Anderson, T. H.; Waite, J. H.; Israelachvili, J. N. Adhesion mechanisms of the mussel foot proteins mfp-1 and mfp-3. *Proc. Natl. Acad. Sci. U. S. A.* **2007**, *104* (10), 3782−3786.
(21) Frank, B. P.; Belfort, G. Adhesion of Mytilus edulis foot protein 1 on silica: Ionic effects on bifouling. *Biotechnol. Prog.* **2002**, *18* (3), 580−586.
(22) Lu, Q.; Danner, E.; Waite, J. H.; Israelachvili, J. N.; Zeng, H.; Hwang, D. S. Adhesion of mussel foot proteins to different substrate surfaces. *J. R. Soc. Interface* **2013**, *10* (79), 20120759.
(23) Danner, E. W.; Kan, Y. J.; Hammer, M. U.; Israelachvili, J. N.; Waite, J. H. Adhesion of mussel foot protein Mefp-5 to mica: An underwater superglue. *Biochemistry* **2012**, *51* (33), 6511−6518.
(24) Hwang, D. S.; Harrington, M. J.; Lu, Q. Y.; Masic, A.; Zeng, H. B.; Waite, J. H. Mussel foot protein-1 (mcfp-1) interaction with titania surfaces. *J. Mater. Chem.* **2012**, *22* (31), 15530−15533.
(25) Yu, J.; Wei, W.; Menyo, M. S.; Masic, A.; Waite, J. H.; Israelachvili, J. N. Adhesion of mussel foot protein-3 to TiO_2 surfaces: the effect of pH. *Biomacromolecules* **2013**, *14* (4), 1072−1077.
(26) Zeng, H. B.; Hwang, D. S.; Israelachvili, J. N.; Waite, J. H. Strong reversible Fe^{3+}-mediated bridging between DOPA-containing protein films in water. *Proc. Natl. Acad. Sci. U. S. A.* **2010**, *107* (29), 12850−12853.
(27) Wei, W.; Yu, J.; Broomell, C.; Israelachvili, J. N.; Waite, J. H. Hydrophobic enhancement of DOPA-mediated adhesion in a mussel foot protein. *J. Am. Chem. Soc.* **2013**, *135* (1), 377−383.
(28) Cui, S. X.; Yu, J.; Kuhner, F.; Schulten, K.; Gaub, H. E. Double-stranded DNA dissociates into single strands when dragged into a poor solvent. *J. Am. Chem. Soc.* **2007**, *129* (47), 14710−14716.
(29) Li, I. T. S.; Walker, G. C. Single polymer studies of hydrophobic hydration. *Acc. Chem. Res.* **2012**, *45* (11), 2011−2021.
(30) Sonnenberg, L.; Luo, Y. F.; Schlaad, H.; Seitz, M.; Colfen, H.; Gaub, H. E. Quantitative single molecule measurements on the interaction forces of poly(L-glutamic acid) with calcite crystals. *J. Am. Chem. Soc.* **2007**, *129* (49), 15364−15371.
(31) Zhang, Y. H.; Yu, Y.; Jiang, Z. H.; Xu, H. P.; Wang, Z. Q.; Zhang, X.; Oda, M.; Ishizuka, T.; Jiang, D. L.; Chi, L. F.; Fuchs, H. Single-molecule study on intermolecular interaction between C-60 and porphyrin derivatives: Toward understanding the strength of the multivalency. *Langmuir* **2009**, *25* (12), 6627−6632.
(32) Han, X. T.; Qin, M.; Pan, H.; Cao, Y.; Wang, W. A versatile "multiple fishhooks" approach for the study of ligand-receptor interactions using single-molecule atomic force microscopy. *Langmuir* **2012**, *28* (26), 10020−10025.
(33) Liang, J.; Fernandez, J. M. Mechanochemistry: One bond at a time. *ACS Nano* **2009**, *3* (7), 1628−1645.
(34) Dietz, H.; Bertz, M.; Schlierf, M.; Berkemeier, F.; Bornschlogl, T.; Junker, J. P.; Rief, M. Cysteine engineering of polyproteins for single-molecule force spectroscopy. *Nat. Protoc.* **2006**, *1* (1), 80−4.
(35) Zheng, P.; Cao, Y.; Li, H. Facile method of constructing polyproteins for single-molecule force spectroscopy studies. *Langmuir* **2011**, *27* (10), 5713−8.
(36) Hoffmann, T.; Dougan, L. Single molecule force spectroscopy using polyproteins. *Chem. Soc. Rev.* **2012**, *41* (14), 4781−96.
(37) Marszalek, P. E.; Dufrene, Y. F. Stretching single polysaccharides and proteins using atomic force microscopy. *Chem. Soc. Rev.* **2012**, *41* (9), 3523−34.
(38) Zocher, M.; Bippes, C. A.; Zhang, C.; Muller, D. J. Single-molecule force spectroscopy of G-protein-coupled receptors. *Chem. Soc. Rev.* **2013**, *42* (19), 7801−15.
(39) Zoldak, G.; Rief, M. Force as a single molecule probe of multidimensional protein energy landscapes. *Curr. Opin. Struct. Biol.* **2013**, *23* (1), 48−57.
(40) Hong, S.; Yang, K.; Kang, B.; Lee, C.; Song, I. T.; Byun, E.; Park, K. I.; Cho, S. W.; Lee, H. Hyaluronic acid catechol: A biopolymer exhibiting a pH-dependent adhesive or cohesive property for human neural stem cell engineering. *Adv. Funct. Mater.* **2013**, *23* (14), 1774−1780.
(41) Hinterdorfer, P.; Baumgartner, W.; Gruber, H. J.; Schilcher, K.; Schindler, H. Detection and localization of individual antibody-antigen recognition events by atomic force microscopy. *Proc. Natl. Acad. Sci. U. S. A.* **1996**, *93* (8), 3477−3481.
(42) Merkel, R.; Nassoy, P.; Leung, A.; Ritchie, K.; Evans, E. Energy landscapes of receptor-ligand bonds explored with dynamic force spectroscopy. *Nature* **1999**, *397* (6714), 50−53.
(43) Bell, G. I. Models for specific adhesion of cells to cells. *Science* **1978**, *200* (4342), 618−627.
(44) Evans, E.; Ritchie, K. Strength of a weak bond connecting flexible polymer chains. *Biophys. J.* **1999**, *76* (5), 2439−2447.
(45) Popa, I.; Fernandez, J. M.; Garcia-Manyes, S. Direct quantification of the attempt frequency determining the mechanical unfolding of ubiquitin protein. *J. Biol. Chem.* **2011**, *286* (36), 31072−31079.
(46) Dietz, H.; Rief, M. Exploring the energy landscape of GFP by single-molecule mechanical experiments. *Proc. Natl. Acad. Sci. U. S. A.* **2004**, *101* (46), 16192−7.
(47) Hentschel, C.; Wagner, H.; Smiatek, J.; Heuer, A.; Fuchs, H.; Zhang, X.; Studer, A.; Chi, L. F. AFM-based force spectroscopy on polystyrene brushes: Effect of brush thickness on protein adsorption. *Langmuir* **2013**, *29* (6), 1850−1856.
(48) Zhang, Y.; Liu, C.; Shi, W.; Wang, Z.; Dai, L.; Zhang, X. Direct measurements of the interaction between pyrene and graphite in aqueous media by single molecule force spectroscopy: understanding the pi-pi interactions. *Langmuir* **2007**, *23* (15), 7911−5.
(49) Conti, M.; Falini, G.; Samori, B. How strong is the coordination bond between a histidine tag and Ni-nitrilotriacetate? An experiment of mechanochemistry on single molecules. *Angew. Chem., Int. Ed.* **2000**, *39* (1), 215−218.
(50) Schmitt, L.; Ludwig, M.; Gaub, H. E.; Tampe, R. A metal-chelating microscopy tip as a new toolbox for single-molecule experiments by atomic force microscopy. *Biophys. J.* **2000**, *78* (6), 3275−3285.
(51) Zheng, P.; Takayama, S. I. J.; Mauk, A. G.; Li, H. B. Hydrogen bond strength modulates the mechanical strength of ferric-thiolate bonds in rubredoxin. *J. Am. Chem. Soc.* **2012**, *134* (9), 4124−4131.
(52) Dougan, L.; Ainavarapu, K. R.; Genchev, G.; Lu, H.; Fernandez, J. M. A single-molecule perspective on the role of solvent hydrogen bonds in protein folding and chemical reactions. *ChemPhysChem* **2008**, *9* (18), 2836−2847.
(53) Zou, S.; Schonherr, H.; Vancso, G. J. Force spectroscopy of quadruple H-bonded dimers by AFM: dynamic bond rupture and molecular time-temperature superposition. *J. Am. Chem. Soc.* **2005**, *127* (32), 11230−1.
(54) Hervas, R.; Oroz, J.; Galera-Prat, A.; Goni, O.; Valbuena, A.; Vera, A. M.; Gomez-Sicilia, A.; Losada-Urzaiz, F.; Uversky, V. N.; Menendez, M.; Laurents, D. V.; Bruix, M.; Carrion-Vazquez, M. Common features at the start of the neurodegeneration cascade. *PLoS Biol.* **2012**, *10* (5), e1001335.
(55) Skulason, H.; Frisbie, C. D. Direct detection by atomic force microscopy of single bond forces associated with the rupture of discrete charge-transfer complexes. *J. Am. Chem. Soc.* **2002**, *124* (50), 15125−33.
(56) Grandbois, M.; Beyer, M.; Rief, M.; Clausen-Schaumann, H.; Gaub, H. E. How strong is a covalent bond? *Science* **1999**, *283* (5408), 1727−30.
(57) Popa, I.; Berkovich, R.; Alegre-Cebollada, J.; Badilla, C. L.; Rivas-Pardo, J. A.; Taniguchi, Y.; Kawakami, M.; Fernandez, J. M. Nanomechanics of halotag tethers. *J. Am. Chem. Soc.* **2013**, *135* (34), 12762−12771.
(58) Schlierf, M.; Li, H. B.; Fernandez, J. M. The unfolding kinetics of ubiquitin captured with single-molecule force-clamp techniques. *Proc. Natl. Acad. Sci. U. S. A.* **2004**, *101* (19), 7299−7304.

(59) Zheng, P.; Chou, C. C.; Guo, Y.; Wang, Y.; Li, H. Single molecule force spectroscopy reveals the molecular mechanical anisotropy of the FeS_4 metal center in rubredoxin. *J. Am. Chem. Soc.* **2013**, *135* (47), 17783−92.
(60) Hwang, D. S.; Zeng, H.; Lu, Q.; Israelachvili, J.; Waite, J. H. Adhesion mechanism in a DOPA-deficient foot protein from green mussels. *Soft Matter* **2012**, *8* (20), 5640−5648.

dx.doi.org/10.1021/la501189n | *Langmuir* 2014, 30, 4358−4366